The Effect of Hot Isostatic Pressing on Crack Initiation, Fatigue, and Mechanical Properties of Two Cast Aluminum Alloys

T.P. Rich, J.G. Orbison, R.S. Duncan, P.G. Olivero, and R.H. Peterec

(Submitted 8 April 1998; in revised form 15 October 1998)

This article presents the results of an experimental materials testing program on the effect of hot isostatic pressing (HIP) on the crack initiation, fatigue, and mechanical properties of two cast aluminum alloys: AMS 4220 and 4225. These alloys are often used in castings for high temperature applications. Standard tensile and instrumented Charpy impact tests were performed at room and elevated temperatures. The resulting data quantify improvements in ultimate tensile strength, ductility, and Charpy impact toughness from the HIP process while indicating little change in yield strength for both alloys. In addition standard fracture mechanics fatigue tests along with a set of unique fatigue crack initiation tests were performed on the alloys. Hot isostatic pressing was shown to produce a significant increase in cycles to crack initiation for AMS 4225, while no change was evident in traditional *da*/*dN* fatigue crack growth. The data permits comparisons of the two alloys both with and without the HIP process.

Keywords aluminum alloys, crack initiation, fatigue, hot isostatic pressing

1. Introduction

The process of hot isostatic pressing (HIP) has been shown to facilitate the closure and rebonding of cracks and voids in some materials and improve the life of engineering components under repeated and changing loads.

The work presented in this article was undertaken to evaluate the effect of the HIP process upon the material properties that control the life of machine and structural components. In particular, two materials were chosen that are often cast for use in high temperature applications: the aluminum alloys AMS 4220 and 4225. The material properties chosen for study were grouped into two categories: mechanical properties relating to strength and ductility and fatigue and crack initiation properties.

2. Background

Hot isostatic pressing is a material process that developed from several fields of metallurgical production. One of the first applications of HIP was performed by Battelle Laboratories as an alternative to sintering powdered materials. This process, then known as gas pressure bonding, was used for compacting and cladding of nuclear fuel elements. At that time, many of the experimental fuel materials were in a powdered form (Ref 1). This initial work led to the subsequent commercial use of HIP for powdered metal (PM) densification.

T.P. Rich and **J.G. Orbison,** Bucknell University, Lewisburg, PA 17837; **R.S. Duncan,** Certainteed Corporation, Valley Forge, PA; **P.G. Olivero,** Polysurveying, Daphne, AL; and **R.H. Peterec,** SECOR International Inc., Robbinsville, NJ. Contact e-mail: rich@bucknell.edu.

In the 1960s HIP was used to compact other materials in powdered form such as cemented carbides, ceramics, composites, and high-speed tool steels. This new process enabled the creation of complex superalloys and bonding of composite materials previously not producible by existing methods. Hot isostatic pressing has also permitted the manufacture of PM components to near-net-shape dimensions, eliminating the need for forging and rough machining processes in many cases (Ref 2) and reducing porosity of such materials (Ref 3).

By 1970, a joint research project conducted by Battelle and the Aluminum Company of America (Alcoa) applied HIP to improve the quality of castings. In this work, HIP was applied to aluminum-alloy diesel engine piston castings (Ref 2). These results, the first using a systematic, experimental basis, showed that HIP produced a tenfold improvement in the fatigue life of these castings (Ref 4). Additionally, this work showed slight increases in tensile properties and a reduced scatter of material parameters typically associated with castings. The results of this investigation are widely published in literature (Ref 4, 5).

The improvement of the Alcoa castings was apparently a result of reduced porosity produced by HIP. The process "healed" voids that were created during casting, using the densification principles similar to that of sintering applied to PM materials.

Commercial application of HIP for the refinement of castings did not progress significantly until the late 1970s, but it has become a recognized method to improve casting quality. Casting alloys of aluminum, titanium, nickel, and high-strength and stainless steels have been enhanced by the HIP process (Ref 2). Some results show that the material properties of HIP castings approach values attained by their wrought and forged counterparts. In addition, the process has been used to rejuvenate in-service castings (Ref 6, 7), improve weldability (Ref 5), and maximize weld homogeneity (Ref 2).

Overall, the literature reviewed indicates that HIP is a production process that can improve the quality of PM and cast

components. Reference 8 summarizes the benefits of HIP applied to PM and cast components:

- Produces uniform density
- Eliminates porosity
- Improves fatigue properties
- Improves creep properties
- Improves ductility and impact strength
- Decreases scatter of properties
- Produces fine grain size structure (PM)
- Produces densification of difficult to compact powders
- Enables fabrication of composite parts
- Enables recovery of defective parts (rejuvenation)
- Creates materials savings (near-net-shape production)

3. HIP Process Description

The HIP process used for casting refinement is simple in concept (Ref 9). Basically, it is the simultaneous application to a component of high isostatic gas pressure and elevated temperature. Under these conditions, a pressure differential is established between the voids within the component and the external surface. This pressure differential induces a concentrated stress state at each void boundary. Localized stress concentrations, combined with the lowered yield strength at the elevated temperature, cause the voids to collapse. After void collapse, plastic deformation and subsequent creep-related flow occur resulting in contact of the void surfaces (Ref 10). Once the surfaces are in contact, diffusion bonding results, completing the healing process.

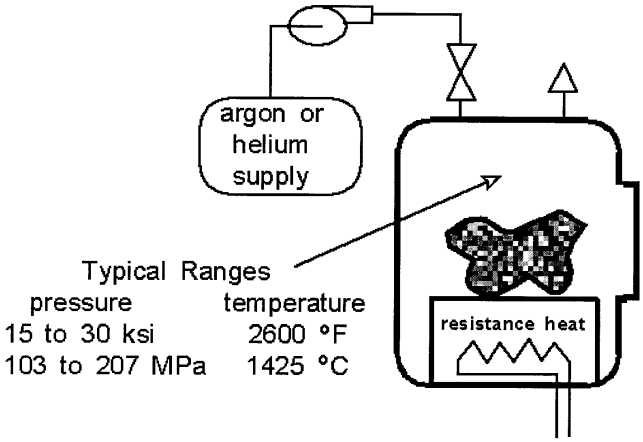

Fig. 1 Schematic of HIP system

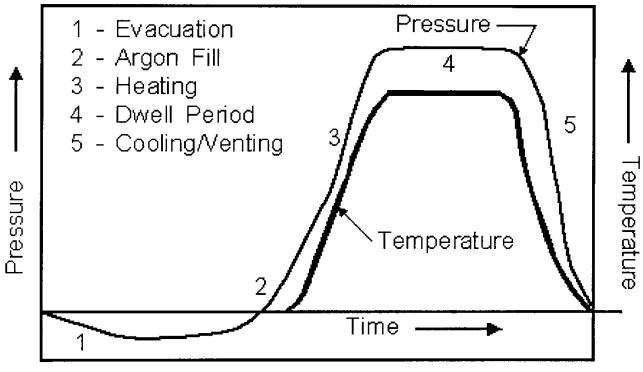

Fig. 2 Typical HIP process diagram

Hot isostatic pressing is performed inside an insulated pressure chamber or autoclave with provisions for external or internal heating and cooling, pressurization piping, and instrumentation. External to the pressure vessel is pressurization and process control equipment, shown schematically in Fig. 1. Inside the pressure vessel, components to be hot isostatically pressed are placed on racks or stands. Components that have pores that interconnect with the surface (e.g., PM materials) are often sealed inside hermetic shells prior to HIP. In some applications, the component is preheated prior to placement in the vessel.

Once the components are in place and the chamber sealed, the chamber is evacuated and then filled with an inert gas, typically argon, or to a lesser degree helium. Inert gases are used so that the component surfaces and chamber walls are protected against harmful effects (such as oxidation or nitriding) during the HIP process. Nitriding has been known to cause extreme surface embrittlement resulting in premature failure of titanium alloy components.

The pressure of the gas is increased to the value specified by the particular HIP application. Typical pressures range from 15,000 to 30,000 psi (103 to 207 MPa) in production presses, while some smaller scale experimental units can be pressurized to 150,000 psi (1,033 MPa). Simultaneously, the temperature inside the chamber is increased to the value determined for the particular application. Once the pressure and temperature reach an equilibrium state (in 0.5 to 4 h), the process is maintained at these parameters for a specified time (dwell times are typically 2 to 6 h, sometimes longer). Figure 2 shows a pressure/temperature/time diagram for a given HIP process (Ref 10).

The governing HIP parameters of pressure, temperature, and time vary, depending upon the applications. These parameters are usually determined experimentally as a function of component geometry, casting quality, and casting alloy. Some typical HIP parameters have been compiled by the General Electric Aircraft Group (Ref 11). For many alloys a 15,000 psi (103 MPa) gas pressure is sufficient. Pressures exceeding 15,000 psi (103 MPa) are only required for alloys that have an extremely high yield strength at elevated temperatures. Hot isostatic pressing at extreme pressures, although costly, has been attempted in order to reduce the required temperature and time parameters. These efforts have not proven to be cost effective (Ref 2).

Hot isostatic pressing temperature is selected to reduce yield strength and promote diffusion bonding. Temperatures typically range from 60 to 90% of the absolute solidus temperature of the alloy. Note that excessive temperatures, while desirable for the HIP process, can have deleterious effects on the microstructure of the alloy (e.g., incipient melting, coarsening of a dispersed phase or precipitate or excessive grain growth). The temperature of the process can also be influenced by the particular heat treatment performed before or after HIP. Finally, the time of the process is mainly a function of the component geometry and the creep and diffusion bonding properties of the

alloy. Generally, time is not extremely critical and can often be set by the production schedule of the particular component.

In summary, HIP appears to be a valid means of improving casting quality by healing of voids. The process is compatible with most casting alloys, and present HIP systems can accommodate components of varying dimensions with little effect on the manufacturing schedule. Hot isostatic pressing parameters of pressure, temperature, and time vary from one application to another; they are usually selected using good engineering judgment and then optimized by sound experimental techniques.

4. Mechanical Testing Studies

4.1 Material Selection and Preparation

The AMS 4220 (3.5 to 4.5% Cu, 1.7 to 2.3% Ni, 1.2 to 1.8% Mg) and AMS 4225 (4.5 to 5.4% Cu, 0.2 to 0.3% Co, 0.2 to 0.3% Mn, 1.3 to 1.7% Ni, 0.2 to 0.3% Sb, 0.15 to 0.25% Ti, and 0.1 to 0.3% Zr) materials were originally received in as-cast form. From that point specific test specimens were produced with the following steps:

- Hot isostatically pressed in as-cast form (except specimens not hot isostatically pressed)
- Heat treated and over aged
- Machined to final dimensions

The HIP process was performed commercially according to the following cycle. After the material was placed into the HIP chamber, the hydrostatic pressure was steadily raised over a 25 to 40 min time period until it reached the HIP pressure of 15,000 psi (103 MPa). Simultaneously the chamber temperature was ramped up to the HIP temperature of 970 °F (521 °C). When both pressure and temperature were stabilized at the HIP values, the material was isostatically pressed for 2 h. Afterward both pressure and temperature were gradually reduced to room conditions over a 35 min period.

All specimen material was heat treated commercially prior to machining. The heat treatment for the AMS 4220 alloy consisted of a solution hardening process with the material held at 960 °F (516 °C) for 5 h, followed by air-blast quenching. The material was then precipitation hardened by reheating to 525 °F (274 °C), maintaining that temperature for 3.5 h, then air cooling. The heat treatment for the AMS 4225 alloy consisted of a solution hardening process with the material being held at 1010 °F (543 °C) for 5 h, followed by a hot water quench at 180 °F (82 °C). The material was then precipitation hardened by reheating to 420 °F (216 °C), maintaining that temperature for 16 h and cooling in air.

4.2 Material Testing Specimens and Procedures

To evaluate the mechanical properties of both alloys at room and elevated temperatures the following tests were performed in accordance with the appropriate ASTM standard:

- Tensile tests ASTM E 8 (Ref 12)
- Brinell hardness ASTM E 10 (Ref 13)
- Charpy impact ASTM E 23 (Ref 14)

Figure 3 shows the exact dimensions of the specimens used in this investigation.

The room temperature tests were conducted at 67 to 70 °F (19 to 21 °C), while the elevated temperature tests were performed at either 445 °F (229 °C) or 575 °F (302 °C).

For the room temperature tensile tests, standard subsize specimens meeting ASTM E 8 requirements were tested in a Baldwin-Southwark universal testing machine with a capacity of 20,000 lb (89 kN). A Tinius-Olsen subsize extensometer (Tinius Olsen Testing Machine Co. Inc., Willow Grove, PA) was used with a 1 in. (25.4 mm) gage length and a least count of 0.0001 in. (0.0025 mm). Elongations were recorded at 100 lb (445 N) increments until the yield strength was approached, then at 50 lb (222.5 N) load increments for the remainder of the extensometer travel.

At elevated temperatures nonstandard subsize tension specimens were tested in an Instron computer-controlled servohydraulic testing system (Instron-Dynatup Corp., Canton, MA) with a maximum capacity of 50,000 lb (222 kN), and an actual load cell capacity of 5,000 lb (22.2 kN). The specimen was specifically designed to meet the requirements of the heating and control systems and consisted essentially of a standard subsize tension specimen meeting the requirements of ASTM E 8, with shoulder sections between the reduced diameter section and the threaded ends. The specimen had a reduced section diameter of 0.250 in. (6.35 mm) (Fig. 3).

The elevated temperature apparatus used for the load frame consisted of pullrods, threaded grips, and a cooling fan. The heating and temperature control apparatus used for the speci-

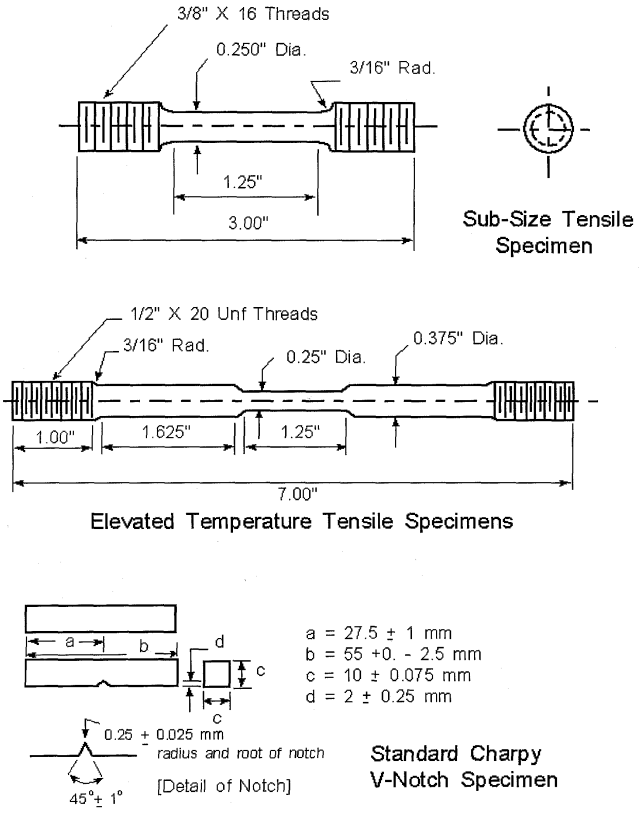

Fig. 3 Materials test specimens

men consisted of resistance heating tape in two circuits, an electronic temperature control unit for each circuit, a single thermocouple, and a voltage controller. A single thermocouple was attached to the specimen surface in the center of the reduced section (center of the actual gage length) and was connected to the temperature controller units for heat tape control. A strain-gage extensometer was then installed on the specimen. When properly assembled, the apparatus produced highly accurate temperature control at the specimen, with worse-case fluctuations not exceeding 5 °F (2.8 °C) above and below the highest target temperature of 575 °F (302 °C). Load control at a rate of 2 lb/s (8.9 N/s) was employed through a strain of 1.0% at which time stroke control, at a rate of 0.000005 in./s (0.000127 mm/s) was used through specimen rupture.

Standard Charpy V-Notch ASTM Type A specimens were tested in a Dynatup instrumented drop-weight impact system (Instron-Dyantup Corp., Canton, MA). Impact velocities averaged 9.35 ft/s (2.85 m/s). These specimens were tested also at three different temperatures: 67, 445, and 575 °F (19, 229, and 302 °C). The elevated specimen temperatures were achieved with an oven; oven temperatures were monitored with a separate digital thermometer with a type K thermocouple. This apparatus is accurate within 3 ° at 575 °F (1.67° at 302 °C) and is more accurate at the lower temperatures.

Specimens for the elevated temperature tests were held precisely at the test temperature for a minimum of 10 min in the oven, most were held at the test temperature for at least 30 min. All were held near the test temperature for at least 30 min; they were tested within 6 s of removal from the oven.

Brinell hardness tests were performed at room temperature on randomly selected Charpy impact specimens after impact testing. Hardness tests were performed a minimum of 10 mm away from the impact failure surface and were distributed over the specimen surface.

4.3 Mechanical Testing Results

Table 1 gives test results. From these results comparisons can be made from one alloy to another, from non-HIP to HIP, and from room temperature to elevated temperatures. Note that test data were obtained on the AMS 4225 at room temperature from two separate batches of material that were processed and tested approximately one year apart. Figure 4 shows typical stress-strain curves for both alloys at each temperature and HIP condition.

The following observations were made from the results of these tests:

- The HIP treatment appears to have little effect on the yield strength (σ_Y, at any temperature). The hardness data reflect this trend.
- The HIP treatment appears to increase ultimate strength and ductility in both alloys at room temperature. At elevated temperatures, however, the HIP treatment appears to have little effect on the ultimate strength of either alloy.

Table 1 Mechanical testing results

Temperature, °F (°C)	HIP or non-HIP	Specimens	Elastic modulus, *E*, ksi (GPa)	Yield strength, ksi (MPa)	Ultimate Tensile strength, ksi (MPa)	Area reduction, *RA*, %	Brinell hardness, HB_{500}, kg/mm^2	Charpy energy, C_V, ft/lb (J)
AMS 4225								
67-70 (19-21)	Non-HIP	2	10,550 (72.74)	32.90 (227)	37.49 (258)	1.6	…	…
		2	…	…	…	…	90.9	0.544 (0.738)
	HIP	3	11,000 (75.84)	31.80 (219)	41.22 (284)	3.0	…	…
		2	…	…	…	…	94.7	0.761 (1.032)
		5(a)	10,500 (72.40)	31.30 (216)	41.60 (287)	2.1	…	…
		…	…	…	…	…	98.7	0.701 (0.950)
445 (229)	Non-HIP	2	7,850 (54.12)	22.80 (157)	23.84 (164)	4.7	…	…
		3	…	…	…	…	…	0.498 (0.675)
	HIP	3	7,600 (52.40)	21.27 (147)	22.99 (159)	21.4	…	…
		3	…	…	…	…	…	0.612 (0.830)
575 (302)	Non-HIP	2	6,300 (43.44)	12.50 (86)	13.18 (91)	16.3	…	…
		5	…	…	…	…	…	0.721 (0.978)
	HIP	2	6,550 (45.16)	13.15 (91)	13.88 (96)	37.3	…	…
		4	…	…	…	…	…	0.687 (0.931)
AMS 4220								
67-70 (19-21)	Non-HIP	1	10,300 (71.02)	14.50 (100)	23.56 (162)	3.1	…	…
		2	…	…	…	…	58.9	1.416 (1.920)
	HIP	2	10,500 (72.40)	14.65 (101)	30.54 (211)	5.5	…	…
		2	…	…	…	…	60.0	1.691 (2.293)
445 (229)	Non-HIP	2	8,400 (57.92)	14.95 (103)	19.55 (135)	22.3	…	…
		3	…	…	…	…	…	1.387 (.1.881)
	HIP	3	8,400 (57.92)	13.73 (95)	18.19 (125)	54.8	…	…
		5	…	…	…	…	…	1.794 (2.432)
575 (302)	Non-HIP	2	7,200 (49.64)	11.20 (77)	13.56 (93)	48.7	…	…
		3	…	…	…	…	…	1.386 (1.879)
	HIP	2	6,900 (47.57)	11.40 (79)	14.02 (93)	77.6	…	…
		3	…	…	…	…	…	1.867 (2.531)

(a) Data from a separate melt.

- The HIP treatment significantly increases ductility in both alloys at all test temperatures.
- Both alloys exhibited a brittle failure mode at room temperature with little area reduction.
- The AMS 4220 alloy, both with and without the HIP treatment, showed a relatively constant yield strength from room temperature through 445 °F (229 °C). However, the ultimate strength was reduced at both elevated test temperatures.
- The AMS 4225 alloy, both with and without the HIP treatment, showed a significant decrease in both yield and ultimate strengths at the elevated test temperatures.
- The yield and ultimate strengths of the two alloys, with and without the HIP treatment, were similar at 575 °F (302 °C). The AMS 4220 alloy showed consistently higher ductility at all test temperatures than the AMS 4225 alloy.
- At both elevated temperatures, significant necking of the specimens was observed in all four groups. At these temperatures, the rupture strength was significantly less than the ultimate tensile strength in all four groups.
- At room temperature, the increased ductility produced by the HIP treatment increased the strain range over which strain hardening occurs. The HIP treatment appears to have little effect on the rate of strain hardening. The increase in strain hardening range appears to produce the higher ultimate tensile strengths seen at room temperature in both alloys.
- At elevated temperatures in all four groups, the ultimate tensile strength was reached relatively soon after yielding (consistent with the room temperature results). At elevated temperatures, the HIP treatment primarily enhanced ductility after the ultimate strength had been reached.

Figure 5 shows typical data from the instrumented Charpy tests. The following observations were made:

- Fracture surfaces on all specimens (both alloys, with and without the HIP treatment, and at all test temperatures) showed 100% brittle fracture, with no evidence of ductility under impact loading.
- The AMS 4220 alloy showed significantly higher energies, at all test temperatures with and without the HIP treatment, than the AMS 4225 alloy. This is consistent with the higher quasistatic ductility shown by the AMS 4220 alloy in the tension tests.
- The HIP treatment increased the impact energy capacity of the AMS 4220 alloy at all temperatures. Further, the HIP treatment of this alloy appears to produce increasing impact energies with increasing test temperature, while the alloy specimens without the HIP treatment showed essentially constant impact energies throughout the test temperature range.

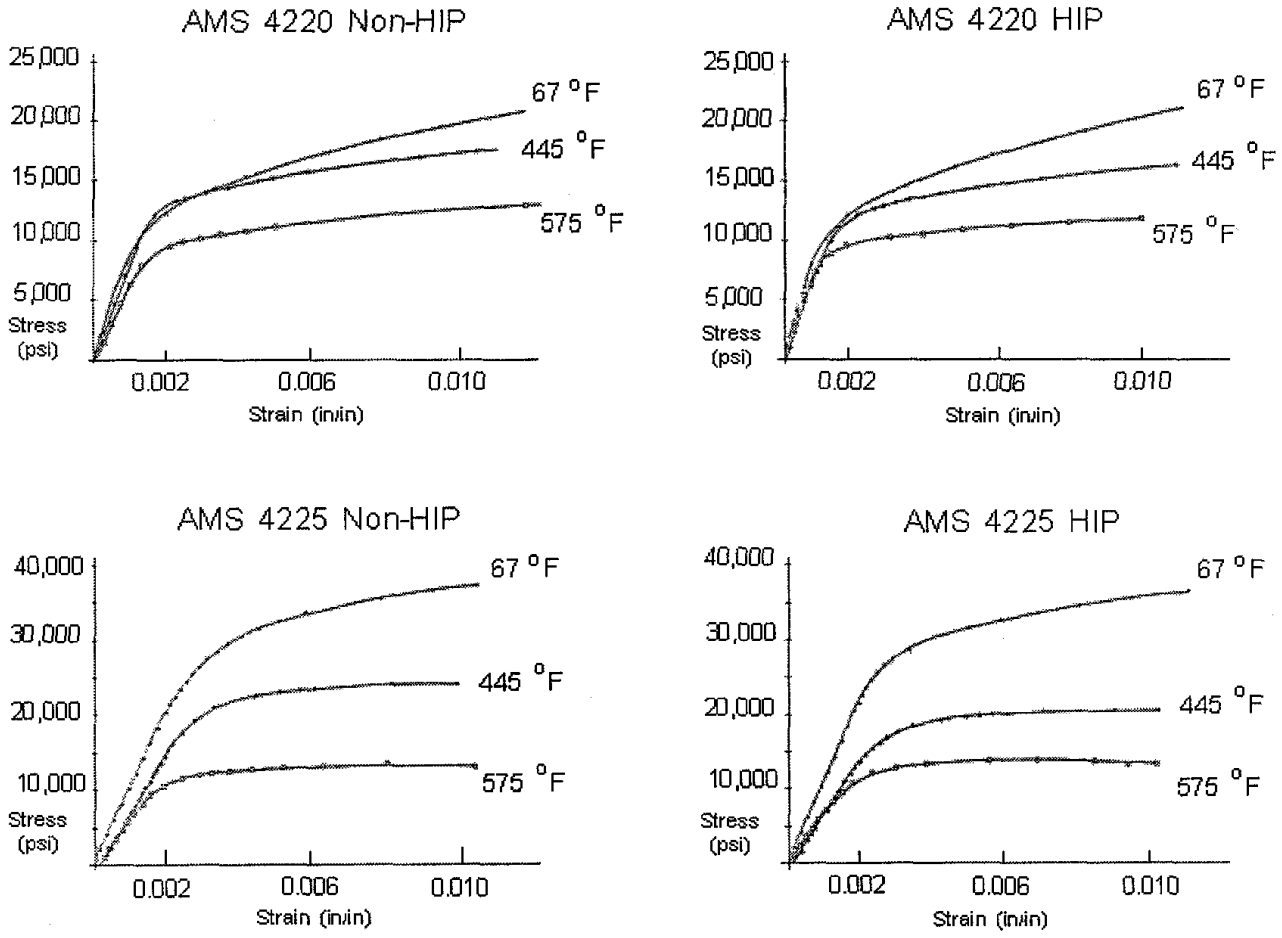

Fig. 4 Typical stress-strain curves

- The AMS 4225 alloy showed an increase in impact energy at the 575 °F (302 °C) test temperature only without the HIP treatment. The HIP treatment of this alloy appears to slightly increase impact energies at room temperature and at 445 °F (229 °C), but has essentially no effect at the 575 °F (302 °C) test temperature.

5. Fatigue and Crack Initiation Studies

The results at room temperature from the mechanical testing studies generally agree with the trends published for another cast aluminum alloy (Ref 4, 5). However, the modest increase in toughness caused by the HIP process cannot account for the reported significant and dramatic increases in the fatigue life measured in previous S-N or actual component life cycle performance testing. Therefore, a second set of tests was performed to characterize the behavior of the aluminum alloys during stable fatigue crack propagation and crack initiation. The following section describes the testing and reveals that it is in the crack initiation phase of crack growth that the HIP process has its most significant effect upon material/component life.

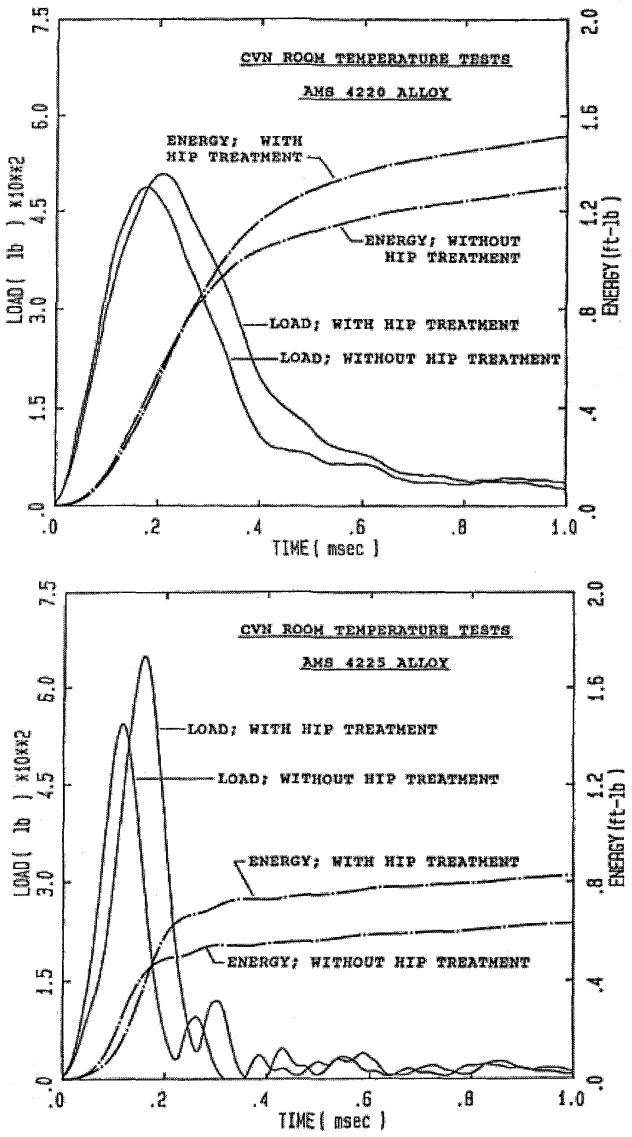

Fig. 5 Typical instrumented Charpy curves

5.1 Fatigue Tests

ASTM E 647 (Ref 15) standard fracture mechanics-based fatigue tests were conducted by a professional materials testing firm on the AMS 4225 aluminum alloy casting material in both the non-HIP and HIP conditions, as defined before. A total of seven non-HIP and nine HIP specimens were tested under controlled sinusoidal loading with load ratios (R factors) in each test set at 0.05, 0.10, or 0.50. Compact tension specimens were employed with overall dimensions of 1.25 in. wide, 1.2 in. high, and 0.25 in. thick (31.75 mm wide, 30.48 mm high, and 6.35 mm thick). Figure 6 shows a composite of the resulting data for the case of R = 0.10; the extreme data points for all of the 0.10 tests are included in this composite. The data for R = 0.05 fell also within this range, and the data for the R = 0.50 fell slightly to the left. No significant difference was observed between the non-HIP and the HIP specimens under any of the testing conditions. Thus, any improvement to the fatigue life of ASM 4225 as a result of HIP must come from the crack initiation phase of crack growth in a component.

5.2 Crack Initiation Tests

In order to evaluate the effect of the HIP process upon the ability of the aluminum alloy to resist the development of macroscopic cracks under a cyclic loading, two questions were addressed: (a) When is a crack a macrocrack? and (b) What experimental system can detect the initiation of a macrocrack? After surveying the various nondestructive testing techniques and systems currently available for flaw detection, an optical experimental system similar to that developed by Papirno and Parker (Ref 16) was selected. Reference 17 gives the specific details relating to the components of the optical detection

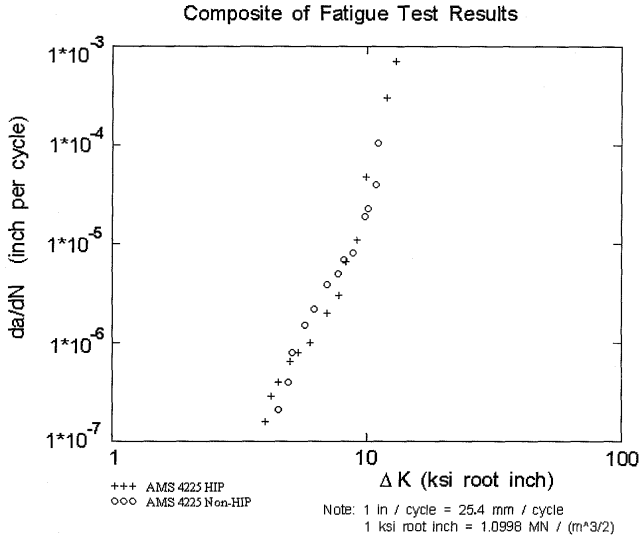

Fig. 6 Typical results from the fracture mechanics-based fatigue tests

system and the development of a compatible compact tension test specimen. It should be noted that no standard test for crack initiation now exists.

There is a coupling between the answers to the two questions posed. In a given materials test specimen or engineering machine component, it can be assumed that microscopic flaws exist such as crystalline dislocations, grain boundaries, inclusions, and larger voids resulting from casting. If a crack is defined at that level, then all material has cracks initiated during the creation of the material. However, if an initiated macrocrack is defined to be a crack larger than the microscopic defects and the result of the migration of microscopic defects to a critical site in the material, then such a crack is defined to exist positively when it can be detected. Thus the practical definition of a macrocrack is limited by the resolution of the experimental detection system.

Figure 7 shows schematically the method of crack detection used in this work. An automated camera with a macro lens and bellows was focused on the root of a notched compact tension specimen. Figure 8 gives the dimensions of the test specimen. Note that the specimen with the smaller ligament size was used in situations where fretting fatigue damage was detected at the pinhole in a prior test. This smaller size reduces the load needed to reach the desired stress concentration in the notch. The fretting damage would have to extend well across the specimen to have a significant effect (>5%) on the crack initiation results (Ref 17). However, the smaller size was used in cases that were found to have some fretting. The specimens were loaded sinusoidally at 10 or 30 Hz at room temperature in an Instron, computer-controlled servohydraulic dynamic testing machine. The loads were kept in tension and controlled such that the maximum tangential stress at the root of the notch was 90% of the yield strength of the material.

Prior to testing, the notches in the machined specimens were carefully polished with 320, 400, and 600 grit emery paper and polishing compound. The polishing direction was circumferential. The polished surface reduced any residual stresses caused by machining and permitted a clearer field of view for the camera system.

Once the loading sequence began, the camera system was automatically triggered to photograph the field of view at preset intervals, usually every 1000 cycles. Each picture was taken at peak load during a given cycle in order to show any macrocracks at maximum opening. The result was a series of photographs showing the root of the notch at an increasingly higher number of load cycles. Once a macrocrack initiated somewhere in the 0.10 in. (2.54 mm) cross section of the root of the notch and grew completely across the thickness, a fully initiated through crack existed and propagated across the ligament of the compact tension specimen in the fashion of a traditional *da*/*dN* fatigue test. This appeared as a 100% through-thickness crack on the photographs, shown in the last photo-sketch No. 110 of Fig. 7. Figure 9 shows a sample photograph. Tracing backward from this point through the photographs revealed the history of the development of the through crack, and a specific level of crack damage was associated with the corresponding load cycles in each photograph. In this manner for each specimen a photograph was sought that had the

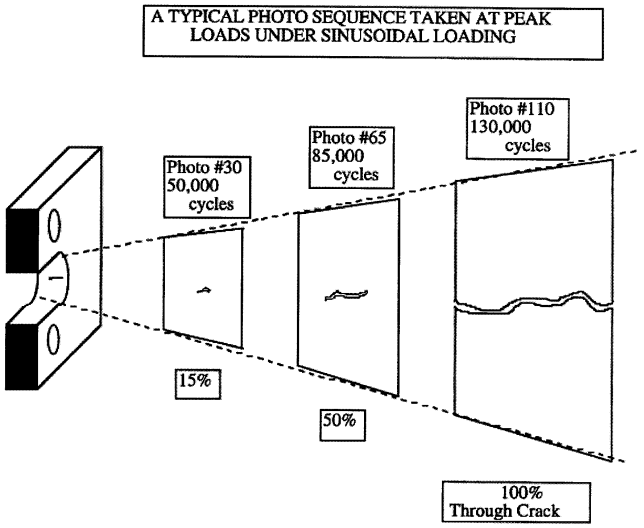

Fig. 7 Crack damage progression through field of view during cyclic loading

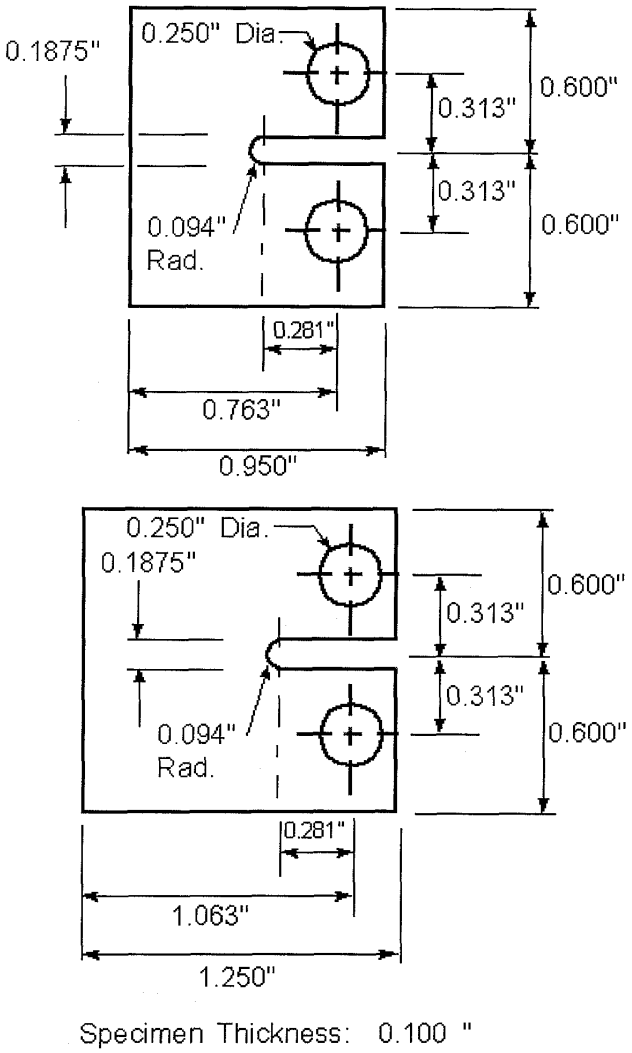

Fig. 8 Fatigue crack initiation specimens

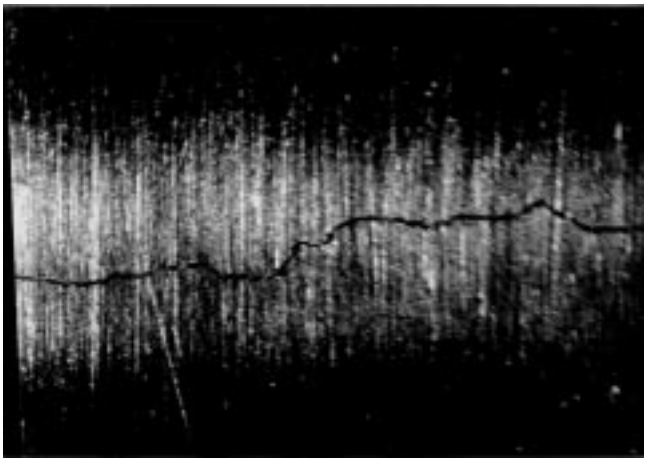

Fig. 9 Photograph of the notch root with a through crack

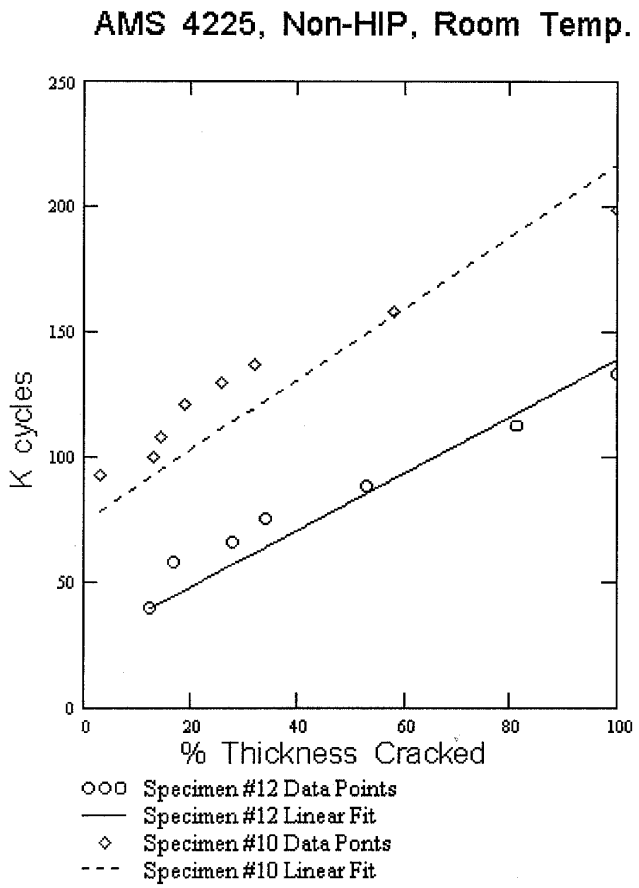

Fig. 10 Crack initiation damage through specimen thickness

smallest visible cracklike marking that eventually grew to the through crack. At that point the prior photograph showed no cracklike markings. (It was easier to conduct this process with the negatives than the actual photos.)

The smallest macrocrack detected via this approach from the data presented in this paper measured 0.0028 in. (0.071 mm) in length. Thus the definition of a macrocrack in this work is a detectable crack that measured nominally 0.003 in. (0.076 mm) and eventually grew to be the dominant through-thickness crack. With this definition, a means for comparison of the crack initiation performance of the AMS 4225 alloy was established.

6. Crack Initiation Results

Extensive crack initiation testing was conducted for the AMS 4225 alloy at room temperature for both non-HIP and HIP material. Table 2 gives the results of the tests. There was significant scatter in the number of cycles estimated to initiate a 0.003 in. (0.076 mm) crack in the non-HIP, AMS 4225 specimens. This had several implications regarding the reduction of the photographic data and the interpretation of the crack initiation mechanism in the compact tension specimens.

First, the scatter in the crack initiation data led to several situations where the macrocracks had begun to grow through the specimens before the first photograph in the given test sequence had been triggered. As a result, the minimum sized crack photographed in a given sequence nearly always exceeded the nominal 0.003 in. (0.076 mm) size. In fact, Table 2 gives the minimum size of the cracks as first photographed for the eight non-HIP specimens. Two specimens (No. 10 and 12) were tested with a photographic record running from small crack sizes, 0.0028 and 0.010 in. (0.071 and 0.254 mm), respectively, all the way to through-thickness cracks. Data from these two records were used in a linear curve fit to find the average slope of the crack growth data (1.284% thickness cracked per K cycle), as shown in Fig. 10. This average slope was then used to extrapolate from the observed minimum-sized crack data observed in the other tests back to the number of cycles estimated to initiate a 0.003 in. (0.076 mm) crack in each individual specimen. Table 2 reports this extrapolated crack initiation data.

Figure 10 also shows a plot of the crack growth data over the full range of specimen thickness for No. 10 and 12. When the data from specimen 10 was extrapolated to initiate a 0.003 in. (0.076 mm) macrocrack, a value of 93.6 K cycles was obtained. For specimen 12 the corresponding value was 44.1 K cycles. This may mean that some original random distribution of microscopic flaws such as casting voids near the surface of the notch in specimen 12 was more severe than in specimen 10 and hence led to a 0.003 in. (0.076 mm) macrocrack in about one-half the number of cycles as in specimen 12.

The linear curve fit reflects the growth of the macrocracks across the specimen notch thickness after initiation of the 0.003 in. (0.076 mm) crack. It appears that once macrocracks were initiated in the specimens the rate of development to through cracks was consistent from specimen to specimen. Hence the average slope of the linear fit was deemed reasonable to back extrapolate the estimated crack initiation cycles for all eight specimens, as given in Table 2.

Table 2 shows the range of scatter evident for the crack initiation cycles for the non-HIP specimens. Even with the uncertainties present in estimating the crack initiation cycles, the average value of 57.4 K cycles and a standard deviation of ±23.4 K cycles appears reasonable for AMS 4225 non-HIP specimens for comparison with the HIP specimens.

Table 2 also presents the results of the crack initiation tests on the HIP specimens. The first two specimens were run to the

Table 2 Crack initiation findings

Specimen identification	AMS 4225 non-HIP crack initiation specimen tests: First photographed macrocrack, in. (mm)	Through thickness, %	Corresponding K cycles at 10 Hz	AMS 4225 non-HIP estimated K cycles to 0.003 in. macrocrack	AMS 4225 HIP K cycles
2	0.050 (1.27)	50	122.4	62.0	499.8
4	0.040 (1.02)	40	96.0	48.5	1,094.3
5	0.005 (0.13)	5	87.9	85.3	10,000.0
7	0.015 (0.38)	15	35.8(a)	20.4	10,000.0(a)
9	0.020 (0.51)	20	70.0	48.2	10,000.0(a)
10	0.0028 (0.07)	2.8	93.3	93.6	…
12	0.010 (0.25)	10	53.1	44.1	809.0(b)
14	0.020 (0.51)	20	79.0	57.2	445.0(b)
Total				8 specimens, average 57.4, standard deviation 23.4	7 specimens

AMS 4220 Non-HIP (one 10 Hz and one 30 Hz). Two specimens ran to 10,000.0 K cycles with no 0.003 in. (0.076 mm) crack. (a) 30 Hz. (b) Through crack

number of cycles shown with no apparent macrocracks. These tests were terminated at that point due to computer malfunctions. The next three specimens each ran for 10,000 K cycles with no detectable macrocracks. These five tests would appear to identify the value of the HIP process to the enhancement of the fatigue life of AMS 4225 components, namely a much extended crack initiation life. However, some doubt still lingers as reflected in the last two specimens reported in the AMS 4225 HIP column. Because of the apparent long life of the HIP specimens the photographic system was not activated. During routine intermittent visual inspection of the notches of these specimens, through cracks were observed at 809.0 and 445.0 K cycles, respectively. Clearly the HIP process did not boost these specimens into the 10,000,000 cycle range. Whatever microscopic defects were present in these two notch surfaces, they were not completely healed by the HIP process. However, they still ran measurably past the 57.4 K cycle level of the non-HIP specimens.

Finally two specimens made from the AMS 4220 in the non-HIP condition were tested for crack initiation. Both specimens lasted to 10,000 K cycles with no macrocracks observed. At this point the crack initiation testing was halted and no HIP specimens were tested because evidence of improvement over the 10,000,000 cycles of the non-HIP case was not sought.

It should be noted that, during testing, very fine multiple cracking was observed on the surfaces of the test specimens similar to that reported by Papirno (Ref 16). Similar to Papirno's observations, these fine cracks did not lead to macrocracks that grew to dominant through cracks in the specimens.

7. Conclusions

The following conclusions were drawn from this study:

- It seems evident that the HIP process can produce significant changes in the size and distribution density of internal voids, and this in turn can alter the mechanical properties of the cast aluminum alloys under study.
- The HIP treatment increases ductility, ultimate tensile strength, impact energy, and to a more variable extent, the service life as related to crack initiation.
- The process produces virtually no change in yield strength and fatigue crack growth rates once initiation has occurred.
- The AMS 4220 alloy displays significantly lower yield and ultimate strengths at room temperature than the AMS 4225 alloy. However, these differences decrease with increasing test temperature and essentially vanish at operating temperatures approaching 575 °F (302 °C).
- The AMS 4220 alloy, again in comparison with the AMS 4225 alloy, is considerably more ductile, has a greater impact energy absorption capacity, and appears to have a more dependable service life to crack initiation.

References

1. E. Bayer, HIP-Tool Materials, *Powder Metall., Int.*, Vol l6 (No. 3), May 1984, p 117-120
2. D.R. Dreger, Healing Defects by HIP, *Mach. Des.*, Vol 53 (No. l2), May 1982, p 79-85
3. A.D. Panasyuk, V.R. Maslennikova, V.G. Kayuk, A.A. Belkina, and A.B. Belykh, Use of Hot Isostatic Pressing to Improve the Properties of Hard Alloy KKhN25, *Powder Metall. Metal Ceram.*, Vol 35 (No. 11-12), 1996, p 644-646
4. R.R. Irving, Hipping is One Way to Check Porosity in Cast Components, *Iron Age*, Vol 225 (No. 33), Nov 1982, p 43-45
5. G.M. Glenn, Improved Properties in Castings by Hot Isostatic Pressing, *SAMPE Q.*, Vol 8 (No. l), Oct 1976, p 1-9
6. P.H. Floyd, W. Wallace, and J. Immarigeon, "Rejuvenation of Properties in Turbine Engine Hot Section Components by Isostatic Pressing," No. 605, Can. Nat. Res. Coun. Lab., Feb 1981
7. A.J. Fletcher, S. King, B. Rickinson, and H. Atkinson, "Effect of Hot Isostatic Pressing on the Mechanical Properties and Microstructure of 70-30 Cupronickel Castings, *Mater. Sci. Technol.*, Vol 9 (No.7), July 1993, p 555-561
8. A Review of the Technology and Applications of Hot Isostatic Pressing of Castings, *Foundry Trade J.*, Vol l54 (No. 3257), Feb 1984, p 228-230
9. N.L. Loh and K.Y. Sia, An Overview of Hot Isostatic Pressing, *J. Mat. Process. Technol.*, Vol 30 (No. 1), Feb 1992, p 45-65
10. H.D.B. Raes, Hot Isostatic Pressing Technology, *Powder Metall.*, Vol 26 (No. 4), April 1983, p 193-199
11. J.C. Bittence, HIP, The Great Healer of Castings, *Mech. Eng.*, Vol 88 (No. 4), Oct 1978, p 54-57
12. "Standard Methods for Tension Testing Metallic Materials," ASTM Standard E 8, 1983

13. "Standard Test Methods for Brinell Hardness of Metallic Materials," ASTM Standard E 10, 1984
14. "Standard Methods for Notched Bar Impact Testing of Metallic Materials," ASTM Standard E 23, 1982
15. "Standard Test Method for Constant-Load Amplitude Fatigue Crack Growth Rates Above 10-8 Meter/Cycle," ASTM Standard E 647, 1983
16. R. Papirno and B.S. Parker, An Automatic Flash Photomicrographic System for Fatigue Crack Initiation Studies, *ASTM Special Technical Publication 519*, 1973, p 98-108
17. J.G. Orbison, R.H. Peterec, J.A. Carhart, and T.P. Rich, Specimen and Automated Test Method Development for Investigation of Fatigue Crack Initiation, *Finite Elem. Anal. Des.*, Vol 10, 1991, p 9-25